Using Torque-Angle and Torque- Velocity Models to Characterize Elbow Mechanical Function: Modeling and Applied Aspects

Diane Haering, Charles Pontonnier, Nicolas Bideau, Guillaume Nicolas, Georges Dumont

USING TORQUE-ANGLE AND TORQUE-VELOCITY MODELS TO CHARACTERIZE ELBOW MECHANICAL FUNCTION: MODELING AND APPLIED ASPECTS

Haering, Diane[1]
IBHGC, ENSAM ParisTech, F-75014 Paris, France

diane.haering@gmail.com

Pontonnier, Charles
Univ Rennes, CNRS, INRIA, IRISA, UMR6074, F-35000 Rennes.

charles.pontonnier@ens-rennes.fr

Bideau, Nicolas
Univ Rennes, M2S, EA1274, F-35000 Rennes.

nicolas.bideau@univ-rennes2.fr

Nicolas, Guillaume
Univ Rennes, M2S, EA1274, F-35000 Rennes.

guillaume.nicolas@univ-rennes2.fr

Dumont, Georges
Univ Rennes, CNRS, INRIA, IRISA, UMR6074, F-35000 Rennes.

georges.dumont@ens-rennes.fr

[1] Corresponding author

ABSTRACT

Characterization of muscle mechanism through the torque-angle and torque-velocity relationships is critical for human movement evaluation and simulation. In-vivo determination of these relationships through dynamometric measurements and modelling is based on physiological and mathematical aspects. However, no investigation regarding the effects of the mathematical model and the physiological parameters underneath these models was found. The purpose of the current study was to compare the capacity of various torque-angle and torque-velocity models to fit experimental dynamometric measurement of the elbow and provide meaningful mechanical and physiological information. Therefore, varying mathematical function and physiological muscle parameters from the literature were tested. While a quadratic torque-angle model seemed to increase predicted to measured elbow torque fitting, a new power-based torque-velocity parametric model gave meaningful physiological values to interpret with similar fitting results to a classical torque-velocity model. This model is of interest to extract modeling and clinical knowledge characterizing the mechanical behavior of such a joint.

.

Keywords: maximal joint torque - isokinetic dynamometer – torque-angle-velocity relationship, maximal power velocity, muscle mechanics.

INTRODUCTION

Joint strength models are valuable representations of the torque generation capacities of a human, useful in direct assessment as well as in musculoskeletal modeling and analyses of human body. These models assume that muscles are viscoelastic actuators [1-3], resulting at the joint level in Joint Torque-Angle and Torque-Velocity Relationships (JTAR and JTVR respectively, and their coupling JTAVR). Fitting such models to specific subjects while keeping their physiological meaning relevant remains an issue. Basically, models are fitted to isokinetic measurements of joint torques in different angle and angular velocity conditions [1–3].

At sarcomere scale, force-length relationship is asymmetrical piecewise linear due to actin and myosin cross-bridge dynamics [4]. At muscle scale, the inter-fiber variability blurs the transient states [5]. At joint scale, muscle-specific non-linear moment arms [6] bring additional transformation into the torque-angle relationship. These observations make it difficult to choose between various JTAR models, and no consensus exists in the literature: normal curve [7,8], quadratic spline [9,10], cubic spline [11], cosinus wave [12], or sinus exponential wave [13]. In a previous study, differences between those models in fitting experimental isokinetic measures have been observed [14], particularly in the eccentric portion of JTAR, evidencing the interaction between angle and velocity in such models. Meanwhile, JTVR is mostly represented with hyperbolic functions [15,16], although it might not cover all the joint velocity range [17].

JTAR and JTVR integrate parameters supposed to be physiologically meaningful. At joint scale, parameters reflect partially the muscle physiology, even if the joint reflects

the interaction between multiple muscles. For JTAR, maximal isometric torque Γ_{max}, optimal isometric angle α_0, and maximal range of motion RoM, are recurrent parameters. For JTVR, Yeadon et al. 2006 [18] introduced maximal eccentric torque, maximal concentric velocity and technical parameters. Anderson, et al. 2007 [12] added eccentric to concentric force ratio and velocities at 75% and 50% of maximal isometric force within the physiological range. In this last model, the two concentric parameters are dependent; and the model lacks derivative continuity between concentric and eccentric portions that can lead to unrealistic JTAVR fitting to data, particularly exhibiting continuity jumps. As proposed in [19], maximal range of velocity can be useful for JTVR extrapolation in high velocity regions.

Besides models fitting issues, physiological significance is useful for interpretation. For example, maximal strength and muscle compositions are useful in ergonomics [20,21]. In sports, specific velocity at maximal power can be a training focus [22]. In clinics, eccentric to concentric strength ratio is an indicator for pathology [23]. Last, musculoskeletal analysis needs such parameters to calibrate models to subjects [24,25]. A direct in-vivo estimation of these parameters remains an issue, since it requires cadaveric, invasive or expensive measurements [24–27]. Joint strength models are therefore useful to get these values indirectly [12,24,28].

The purpose of the current study is to investigate the effects of mathematical models and muscle parameters on JTAR and JTVR from modeling and applied points of views. We assumed that:

- **[H1]** an asymmetrical JTAR can reduce torque prediction errors;

- **[H2]** a new power-based JTVR can improve the physiological relevance of such models.

METHODS

Ethics and Participants

Under INRIA national ethics committee agreement (COERLE #2017-002), twenty-two male participants (33±6 years; 1.81±0.07 m; 78±9 kg) gave their informed consent to participate in the study.

Isokinetic measurement

Participants seated upright with the arm alongside on a Con-Trex MJ® isokinetic dynamometer (CMV AG, Dübendorf, Switzerland) according the manual guidelines (fig. 1). The dynamometer axis was aligned with the elbow flexion axis at 90° for maximum precision. Maximal distance between handle and arm brace without hampering elbow flexion was chosen to minimize elbow displacement away from the dynamometer axis. Similarly, tight straps were used to immobilize thorax. Range of motion was adjusted to the subject.

Goniometric measurement was used to calibrate angular values. Three passive flexion-extension trials at $60°.s^{-1}$, $120°.s^{-1}$, or $180°.s^{-1}$ were recorded for gravity and passive components compensation.

After a ten minutes sub-maximal warm-up, five voluntary flexion or extension hold for five seconds at angles evenly spaced throughout the range of motion were recorded as isometric trials. Then, three repetitions of concentric-passive cycles at $60°.s^{-1}$, $120°.s^{-1}$, or $180°.s^{-1}$ or eccentric-passive trials at $60°.s^{-1}$, $120°.s^{-1}$, or $180°.s^{-1}$ in flexion and extension

were recorded as isokinetic trials. Within subject ranges of motion, reaching isokinetic state limited the maximal velocity to 180°.s^{-1}. During 180°.s^{-1} trials, subjects were asked to anticipate their effort at the end of the previous passive cycle to decrease delay and ensure a sufficient maximal contraction time during trials. To decrease fatigue effects, trials order was randomized within subjects, flexion and extension trials were alternated, and a 45 seconds rest was respected between each trial. All measurements were collected by the same experimenter. Angle, angular velocity and torque were recorded at 256 Hz. Only data corresponding to isokinetic states were used for analysis, discarding the first milliseconds of trials (215 ms to 355 ms) during which muscle activation is not maximal [18]. For each condition, the repetition with the largest average torque was selected.

INSERT FIGURE 1 HERE

JTAR models

Five JTAR mostly encountered in the literature were implemented as Normal [3,10], Quadratic [11,12], Cosinus [13], Cubic [14] and Sinus-exponential [15] models. Parameters of all these models are the maximal isometric torque Γ_{max}, the optimal joint angle α_0 and the maximal range of isometric force production RoM. These models are extensively described in the supplementary material and presented in figure 2.

INSERT FIGURE 2 HERE

92 **JTVR models**

93 Two JTVR models were compared. The Anderson-based model is an adapted version of
94 [12]. The power-based model is a new polynomial function of the maximal power velocity
95 and other physiological parameters selected from the literature.
96 The Anderson-based model introduces 3 parameters: $\omega_{\Gamma_{.75}}$ - Velocity at 75% of maximal
97 isometric torque , E - Eccentric to concentric torque index and an additional $\omega_{\Gamma_{.5}}/\omega_{\Gamma_{.75}}$
98 ratio as an optimization constraint rather than an arbitrary value as in the original version.
99 The power-based model depends on the concentric velocity at maximal power, $\boldsymbol{\omega_{P_{max}}}$,
100 because of its unique correlation with muscle composition [29,30]. $\boldsymbol{\omega_{P_{max}}}$ is also used as
101 an inflexion constraint for the concentric part of the JTAR. The model also depends on
102 $\omega_{min}/\omega_{max}$ - Max. eccentric to concentric velocity ratio, $\Gamma_{ECC}/\Gamma_{CON}$ - Max. eccentric to
103 concentric torque ratio and $\boldsymbol{\omega_{max}}$ - Maximum concentric velocity at which muscle sustains
104 no more tension [31].
105 Both models are extensively described in the supplementary material and presented in
106 figure 3.
107
108 INSERT FIGURE 3 HERE
109
110 **Fitting models to data**
111 A least-square-curve-fitting method (trust-region algorithm, Matlab® Optimization
112 Toolbox™) minimized the quadratic distance between modelled and measured torques
113 by optimizing models parameters.

Isometric, concentric and eccentric parameters were optimized in successive steps as recommended by [12]. The five JTAR models were tested in the isometric step and were combined with both JTVR models in the 2nd and 3rd steps.

Since range of motion and acquisition rate were constant for all trial, duration and frame number varied for each velocity. To guarantee equal weight of all velocities on fitting, samples of equal number of frames were selected within the algorithm.

Models comparison

First, models were compared in terms of ability to fit data. Adjusted correlation and linear regression coefficients were compared between all combinations of JTAR and JTVR models. Additionally, a one-way repeated measures Anova was performed to test the effects of JTAR models on isometric torque prediction errors; and a two-way repeated measures Anova was performed to test the effects of JTAR and JTVR models on isokinetic (concentric + eccentric) torque prediction errors. Mauchly normality and sphericity test was performed. Then, the Distribution Cumulative Differences (Matlab® Statistics & Machine Learning Toolbox™) was performed for the Anovas. Results are presented with significance level set to $p \leq .05$ and significance power F.

Second, the optimized parameters of all models were compared and confronted to literature values.

RESULTS

The significant effects of JTAR and JTVR were not different between flexion or extension motions. Results for both motions are presented together in this section.

Torque predicted by cosinus, quadratic, and cubic models displayed larger correlation with experimental data than normal and sinus-exponential models (table 1). Highest correlations were obtained for isometric data. Correlation for concentric data was higher with the power-based model than with the Anderson-based model but lower for eccentric data.

INSERT TABLE 1 HERE

Sphericity was verified for all data ($p < 0.01$). ANOVA revealed that JTAR had significant effects on isometric prediction errors ($p < 0.01$, $F = 3.86$). Post-hoc tests attributed the smallest errors to the quadratic model ($p < 0.001$, Fig 4a). Error increased significantly of 0.19, 0.53, 2.67, and 4.25 N.m between cosinus, cubic, sinus-exponential and normal models respectively.

The ANOVA showed an ordinal interaction between these models on average error ($p < 0.01$, $F = 18.36$), plus significant effects of JTAR ($p < 0.01$, $F = 13.15$) and JTVR ($p < 0.05$, $F = 4.66$). Normal and sinus-exponential models still displayed the largest errors - 10% larger than other models - in combination with both JTVR models (Fig. 4b). The power-based model displayed larger overall error than Anderson's model only when combined with sinus-exponential and normal torque-angle models.

INSERT FIGURE 4 HERE

Average isometric parameters obtained with each model are presented in table 2. In flexion, Γ_{max} varied between 63 N.m and 69 N.m, RoM varied between 155° and 175°, and α_0 varied between 59° and 102°. In extension, Γ_{max} between 60 N.m and 66 N.m, RoM between 164° and 179°, and α_0 between 56° and 99° were obtained in extension. Significant effects of the model were found for Γ_{max} and α_0 only in extension ($p < 0.05$, $F = 2.93$, and $p < 0.01$, $F = 3.90$ respectively). Average Γ_{max} obtained with cubic and sinus-exponential models, and average α_0 obtained with the normal model, differed by more than 10% from values found in the literature.

INSERT TABLE 2 HERE

Optimal ω_{max}, ω_{min}, and $\omega_{P_{max}}$ obtained from the new model combined to each isometric model are presented in table 3. No statistical effect of the model was found for these parameters.

INSERT TABLE 3 HERE

Optimal $\Gamma_{ECC}/\Gamma_{CON}$ ratios obtained with both JTVR are presented in table 4. The ANOVA showed an effect of the JTAR, but no effect of the JTVR and an interaction between JTAR and JTVR. Differences identified through the post-hoc tests were about 1% of the average ratio values.

INSERT TABLE 4 HERE

Discussion

The purpose of the current study was to investigate the capacity of JTAR and JTVR models to represent the elbow mechanical function from modeling and applied points of views. We first compared their ability to fit the experimental data and then interpreted their physiological parameters in comparison to the literature.

Differences in fitting experimental data were observed. Both choices of JTAR and JTVR showed statistical effects and interaction on maximal torque prediction. For JTAR, **[H1]** was not verified, since the asymmetrical models displayed significantly larger errors than two of the symmetrical models (quadratic and cosinus). This may be explained by interactions between maximal forces and moment arms of multiple muscles crossing the elbow [6]. For the elbow joint, the quadratic JTAR appears as the most accurate and adaptable model on a large cohort. Those results might be joint-specific. As reported in our preliminary study [14], average prediction error is increased by the JTVR. Associated with one of the two best JTAR (i.e. quadratic, cosinus, cubic), the power-based and Anderson-based models gave similar prediction levels. Although the new physiological parameters may improve the model meaningfulness, it did not improve its compliance to fit measured data. Especially, the additional constraint added to ensure derivative continuity between concentric and eccentric parts of the model seemed to decrease eccentric fitting efficiency of the model. However, it ensured that the torque envelope generated by the fitting method was continuous, that may not be the case with the

Anderson-based one. Globally, correlations between measured and predicted JTAVR were weaker in the current study than in other studies in the literature that focused on lower limbs [14,21]. This result may be due to the larger anatomical variability of the upper limb. Moreover, larger misalignment between elbow and dynamometer axes may arise during motion because of the equipment, since the arm position cannot be as controlled as the thigh on the dynamometer. Quantification and correction of this problem could improve the fitting quality and the subsequent parameter estimation. Specific joint strengths models dedicated to fitting may also have been of interest to be tested here [5,36]

For applied perspectives, physiological parameters obtained through optimization of the models seem coherent with the literature. For a group of young healthy men, maximal isometric torque Γ_{max} between 63 N.m and 69 N.m in flexion [2,32], and balanced flexion-extension ratios between .95 and .97 are similar to literature [2,33]. Range of motion RoM obtained with all models is larger than the anatomical reference [34], probably due to an extrapolation of muscle strength beyond realistic elbow configuration due to bony limits. Average optimal angle, α_0, obtained for elbow flexion and extension with all models are consistent with the literature [35–37]. For both flexion and extension, α_0 found for normal (79°,76°), cosinus (77°,72°), and quadratic (77°,72°) models was close to classically observed average angles [38,39], while cubic (59°,56°) and sinus-exponential (112°,99°) models values were at boundaries. Only Γ_{max} obtained with cubic and sinus-exponential

models, and α_0 obtained with the normal model differed by more than 10% from literature values [32,38].

Concerning concentric and eccentric parameters, concentric velocity at maximal power, $\omega_{P_{max}}$, was our focus. Due to its relationship with muscle composition [30], linking mechanical and physiological muscle functions, the implementation of this parameter in the model seemed interesting for applications in sports, rehabilitation or ergonomics [40]. Optimized $\omega_{P_{max}}$ values, between 404°.s^{-1}, and 561°.s^{-1}, are about two times larger than $\omega_{P_{max}}$ values only based on isokinetic dynamometer for thigh muscles [29]. Previous study showed that measured $\omega_{P_{max}}$ correlated better (r=.55) with fiber composition when corrected with a Hill-type model as in our study [41] and could have values between 215°.s^{-1} and 539°.s^{-1}. Although correlations are seen, only 51.8% of the fiber composition variance was explained by $\omega_{P_{max}}$ [42]. For further work, a combination of $\omega_{P_{max}}$ measurements with Hill-model correction and electromyography could be investigated [43] and a validation of muscle composition prediction through this technique should be performed.

For the other concentric and eccentric parameters, maximal concentric velocity, ω_{max}, between 1268°.s^{-1} and 1531°.s^{-1} in flexion and, 1368°.s^{-1} and 1667°.s^{-1} in extension were found. That lays below values reported for baseball players, middle-aged, and elderly men respectively [43,44] . The normal and sinus-exponential models produced the smallest values. For maximal eccentric velocity, ω_{min}, no conclusive reference data were found. In general, physiological parameters related to velocity were obtained by extrapolation of our model beyond highest velocity measured in this study. Since no direct measurement

for much higher velocities was possible with such dynamometers, these values cannot be directly validated.

Since the degree of meaningfulness of the power-based JTVR was higher, without decreasing significantly the data fitting, **[H2]** seemed verified.

To conclude, five JTAR and two JTVR were compared when fitting experimental dynamometric measurements from modelling and applied perspectives. While a quadratic torque-angle model fitted best the data, a new proposed JTVR increased physiological transparency and clinical relevance without decreasing significantly the data fitting. The study highlights the needs for improvement of dynamometric measurement accuracy for the upper limb and the importance of the meaningfulness of the physiological parameters to be optimized when fitting these models to data.

AKNOWLEDGMENT

The authors want to acknowledge INRIA who funded a post-doctoral scholarship on this project.

CONFLICT OF INTEREST

The authors encountered no conflict of interest for the current study.

REFERENCES

[1] Bosco, C., Belli, A., Astrua, M., Tihanyi, J., Pozzo, R., Kellis, S., Tsarpela, O., Foti, C., Manno, R., and Tranquilli, C., 1995, "A Dynamometer for Evaluation of Dynamic Muscle Work," Eur. J. Appl. Physiol., **70**(5), pp. 379–386.

[2] Frey-Law, L. A., Laake, A., Avin, K. G., Heitsman, J., Marler, T., and Abdel-Malek, K., 2012, "Knee and Elbow 3D Strength Surfaces: Peak Torque-Angle-Velocity Relationships," J. Appl. Biomech., **28**(6), pp. 726–737.

[3] Gülch, R. W., 2008, "Force-Velocity Relations in Human Skeletal Muscle," Int J Sports Med, **15**(S 1), pp. S2–S10.

[4] Cole, G. K., Van Den Bogert, A. J., Herzog, W., and Gerritsen, K. G., 1996, "Modelling of Force Production in Skeletal Muscle Undergoing Stretch," J. Biomech., **29**(8), pp. 1091–1104.

[5] Rassier, D., MacIntosh, B., and Herzog, W., 1999, "Length Dependence of Active Force Production in Skeletal Muscle," J. Appl. Physiol., **86**(5), pp. 1445–1457.

[6] Murray, W. M., Delp, S. L., and Buchanan, T. S., 1995, "Variation of Muscle Moment Arms with Elbow and Forearm Position," J. Biomech., **28**(5), pp. 513517–515525.

[7] Brown, I. E., Cheng, E. J., and Loeb, G. E., 1999, "Measured and Modeled Properties of Mammalian Skeletal Muscle. II. The Effects of Stimulus Frequency on Force-Length and Force-Velocity Relationships," J. Muscle Res. Cell Motil., **20**(7), pp. 627–643.

[8] Zajac, F. E., 1989, "Muscle and Tendon: Properties, Models, Scaling, and Application to Biomechanics and Motor Control," Crit. Rev. Biomed. Eng., **17**(4), pp. 359–411.

[9] Chow, J. W., Darling, W. G., Hay, J. G., and Andrews, J. G., 1999, "Determining the Force-Length-Velocity Relations of the Quadriceps Muscles: III. A Pilot Study," J. Appl. Biomech., **15**(2), pp. 200–209.

[10] van den Bogert, A. J., Gerritsen, K. G., and Cole, G. K., 1998, "Human Muscle Modelling from a User's Perspective," J. Electromyogr. Kinesiol. Off. J. Int. Soc. Electrophysiol. Kinesiol., **8**(2), pp. 119–124.

[11] Lloyd, D. G., and Besier, T. F., 2003, "An EMG-Driven Musculoskeletal Model to Estimate Muscle Forces and Knee Joint Moments in Vivo," J. Biomech., **36**(6), pp. 765–776.

[12] Anderson, D. E., Madigan, M. L., and Nussbaum, M. A., 2007, "Maximum Voluntary Joint Torque as a Function of Joint Angle and Angular Velocity: Model Development and Application to the Lower Limb," J. Biomech., **40**(14), pp. 3105–3113.

[13] Hatze, H., 1977, "A Myocybernetic Control Model of Skeletal Muscle," Biol. Cybern., **25**(2), pp. 103–119.

[14] Haering, D., Pontonnier, C., and Dumont, G., 2017, "Which Mathematical Model Best Fit the Maximal Isometric Torque-Angle Relationship of the Elbow?," Comput. Methods Biomech. Biomed. Engin., **20**(sup1), pp. 101–102.

[15] Brown, I. E., Scott, S. H., and Loeb, G. E., 1996, "Mechanics of Feline Soleus: II. Design and Validation of a Mathematical Model," J. Muscle Res. Cell Motil., **17**(2), pp. 221–233.

[16] van Soest, A. J., Huijing, P. A., and Solomonow, M., 1995, "The Effect of Tendon on Muscle Force in Dynamic Isometric Contractions: A Simulation Study," J. Biomech., **28**(7), pp. 801–807.
[17] Wickiewicz, T. L., Roy, R. R., Powell, P. L., Perrine, J. J., and Edgerton, V. R., 1984, "Muscle Architecture and Force-Velocity Relationships in Humans," J. Appl. Physiol., **57**(2), pp. 435–443.
[18] Yeadon, M. R., King, M. A., and Wilson, C., 2006, "Modelling the Maximum Voluntary Joint Torque/Angular Velocity Relationship in Human Movement," J. Biomech., **39**(3), pp. 476–482.
[19] Forrester, S. E., Yeadon, M. R., King, M. A., and Pain, M. T., 2011, "Comparing Different Approaches for Determining Joint Torque Parameters from Isovelocity Dynamometer Measurements," J. Biomech., **44**(5), pp. 955–961.
[20] Haering, D., Pontonnier, C., Bideau, N., Nicolas, G., and Dumont, G., 2017, "Task Specific Maximal Elbow Torque Model For Ergonomic Evaluation," *Proceedings of the XXVI Congress of the International Society of Biomechanics*.
[21] Moore, J. S., and Garg, A., 1995, "The Strain Index: A Proposed Method to Analyze Jobs for Risk of Distal Upper Extremity Disorders," Am. Ind. Hyg. Assoc. J., **56**(5), pp. 443–458.
[22] Haff, G. G., and Nimphius, S., 2012, "Training Principles for Power," Strength Cond. J., **34**(6).
[23] Hedlund, M., Lindström, B., Sojka, P., Lundström, R., and Olsson, C.-J., 2017, "Pronounced Decrease in Concentric Strength Following Stroke Due to Pre-Frontally Mediated Motor Inhibition," Physiotherapy, **101**, pp. e553–e554.
[24] Muller, A., Haering, D., Pontonnier, C., and Dumont, G., 2017, "Non-Invasive Techniques for Musculoskeletal Model Calibration," *Congrès Français de Mécanique*, Lille.
[25] Staron, R. S., Hagerman, F. C., Hikida, R. S., Murray, T. F., Hostler, D. P., Crill, M. T., Ragg, K. E., and Toma, K., 2000, "Fiber Type Composition of the Vastus Lateralis Muscle of Young Men and Women," J. Histochem. Cytochem. Off. J. Histochem. Soc., **48**(5), pp. 623–629.
[26] Sopher, R. S., Amis, A. A., Davies, D. C., and Jeffers, J. R., 2017, "The Influence of Muscle Pennation Angle and Cross-Sectional Area on Contact Forces in the Ankle Joint," J. Strain Anal. Eng. Des., **52**(1), pp. 12–23.
[27] Veeger, H. E., Yu, B., An, K. N., and Rozendal, R. H., 1997, "Parameters for Modeling the Upper Extremity," J. Biomech., **30**(6), pp. 647–652.
[28] Croisier, J. L., and Crielaard, J. M., 1999, "Exploration Isocinétique: Analyse Des Paramètres Chiffrés," Ann. Réadapt. Médecine Phys., **42**(9), pp. 538–545.
[29] Froese, E. A., and Houston, M. E., 1985, "Torque-Velocity Characteristics and Muscle Fiber Type in Human Vastus Lateralis," J. Appl. Physiol., **59**(2), pp. 309–314.
[30] Schantz, P., Randal Fox, E., Hutchison, W., Tydén, A., and Åstrand, P., 1983, "Muscle Fibre Type Distribution, Muscle Cross-sectional Area and Maximal Voluntary Strength in Humans," Acta Physiol., **117**(2), pp. 219–226.
[31] Hill, A. V., 1938, "The Heat of Shortening and the Dynamic Constants of Muscle," Proc. R. Soc. Lond. B Biol. Sci., **126**(843), pp. 136–195.

[32] Gauthier, A., Davenne, D., Martin, A., and Van Hoecke, J., 2001, "Time of Day Effects on Isometric and Isokinetic Torque Developed during Elbow Flexion in Humans," Eur. J. Appl. Physiol., **84**(3), pp. 249–252.
[33] Ellenbecker, T. S., and Roetert, E. P., 2003, "Isokinetic Profile of Elbow Flexion and Extension Strength in Elite Junior Tennis Players," J. Orthop. Sports Phys. Ther., **33**(2), pp. 79–84.
[34] Boone, D. C., and Azen, S. P., 1979, "Normal Range of Motion of Joints in Male Subjects.," JBJS, **61**(5), pp. 756–759.
[35] Chang, Y.-W., Su, F.-C., Wu, H.-W., and An, K.-N., 1999, "Optimum Length of Muscle Contraction," Clin. Biomech., **14**(8), pp. 537–542.
[36] Koo, T. K. ., Mak, A. F. ., and Hung, L. ., 2002, "In Vivo Determination of Subject-Specific Musculotendon Parameters: Applications to the Prime Elbow Flexors in Normal and Hemiparetic Subjects," Clin. Biomech., **17**(5), pp. 390–399.
[37] Mountjoy, K., Morin, E., and Hashtrudi-Zaad, K., 2010, "Use of the Fast Orthogonal Search Method to Estimate Optimal Joint Angle for Upper Limb Hill-Muscle Models," IEEE Trans. Biomed. Eng., **57**(4), pp. 790–798.
[38] Hasan, Z., and Enoka, R., 1985, "Isometric Torque-Angle Relationship and Movement-Related Activity," Exp Brain Res, **59**, pp. 441–450.
[39] Thomis, M. A., Van Leemputte, M., Maes, H. H., Blimkie, C. J. R., Claessens, A. L., Marchal, G., Willems, E., Vlietinck, R. F., and Beunen, G. P., 1997, "Multivariate Genetic Analysis of Maximal Isometric Muscle Force at Different Elbow Angles," J. Appl. Physiol., **82**(3), p. 959.
[40] Karp, J. R., 2001, "Muscle Fiber Types and Training.," Strength Cond. J., **23**(5), p. 21.
[41] MacIntosh, B. R., Herzog, W., Suter, E., Wiley, J. P., and Sokolosky, J., 1993, "Human Skeletal Muscle Fibre Types and Force: Velocity Properties," Eur. J. Appl. Physiol., **67**(6), pp. 499–506.
[42] Suter, E., Herzog, W., Sokolosky, J., Wiley, J. P., and Macintosh, B. R., 1993, "Muscle Fiber Type Distribution as Estimated by Cybex Testing and by Muscle Biopsy.," Med. Sci. Sports Exerc., **25**(3), pp. 363–370.
[43] Kim, C., Gao, Q., Kim, W., and Kim, W., 1994, "Muscle Fiber Type Distribution Estimated by Non-Invasive Technique: Based on Isometric Force and Integrated Electromyography," Clin. Sci., **87**(s1), p. 107.
[44] Toji, H., and Kaneko, M., 2007, "Effects of Aging on Force, Velocity, and Power in the Elbow Flexors of Males," J. Physiol. Anthropol., **26**(6), pp. 587–592.

388 **Figure Captions List**
389

Fig. 1 Experimental set up. The participant is seated and attached to the ConTrex dynamometer in upright position with the arm along his side. The axis of the dynamometer is aligned with the epicondylitis axis with the elbow flexed at 90°.

Fig. 2 Normalized torque-angle relationship as defined by the five mathematical models: normal, cosinus, and quadratic models are symmetrical; cubic and sinus-exponential are asymmetrical.

Fig. 3 Normalized torque-velocity models and constraint parameters: in the Anderson-based model (A), we find one derivative constraint at ω_{max}, two independent constraints at $-\omega_{max}$ and ω_0, and two dependant constraints at $\boldsymbol{\omega}_{\boldsymbol{\Gamma}_{.5}}$ and $\boldsymbol{\omega}_{\boldsymbol{\Gamma}_{.75}}$; in our power-based model (B), we defined three derivative constraints and three independent constraints at ω_{max}, ω_{max}, and ω_0, and an additional derivative constraints at $\omega_{P_{max}}$ on the power-velocity relationship.

Fig. 4 Effects of torque-angle models (A) and interaction between the torque-angle and torque-velocity models (B) on average prediction errors. Colored stars represent individuals (one color = one subject). Black dots, blue dots and red diamonds represent the average of all individuals. Asterisks indicate significant difference between means.

390
391

392 **Table Caption List**
393

Table 1 Adjusted correlation coefficients between measured and predicted maximal torque for all models in elbow flexion and extension for each type of data: isometric, concentric and eccentric.

Table 2 Optimal elbow torque-angle parameters obtained with the five isometric models.

Table 3 Optimal elbow torque-velocity parameters of the new model obtained with the five isometric models.

Table 4 Optimal elbow eccentric to concentric ratios obtained with Anderson-based model and the new model combined with each of the five isometric models.

394

Figure 1– Experimental set up. The participant is seated and attached to the ConTrex dynamometer in upright position with the arm along his side. The axis of the dynamometer is aligned with the epicondylitis axis with the elbow flexed at 90°.

Figure 2 – Normalized torque-angle relationship as defined by the five mathematical models: normal, cosinus, and quadratic models are symmetrical; cubic and sinus-exponential are asymmetrical.

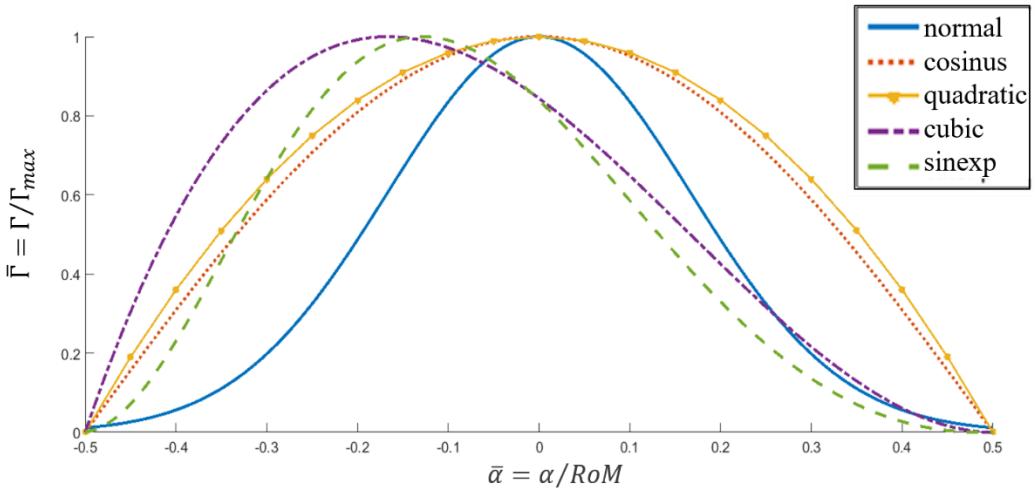

Figure 3 – Normalized torque-velocity models and constraint parameters: in the Anderson-based model (A), we find one derivative constraint at ω_{max}, two independent constraints at $-\omega_{max}$ and ω_0, and two dependant constraints at $\boldsymbol{\omega_{\Gamma.5}}$ and $\boldsymbol{\omega_{\Gamma.75}}$; in our power-based model (B), we defined three derivative constraints and three independent constraints at ω_{max}, ω_{max}, and ω_0, and an additional derivative constraints at $\omega_{P_{max}}$ on the power-velocity relationship.

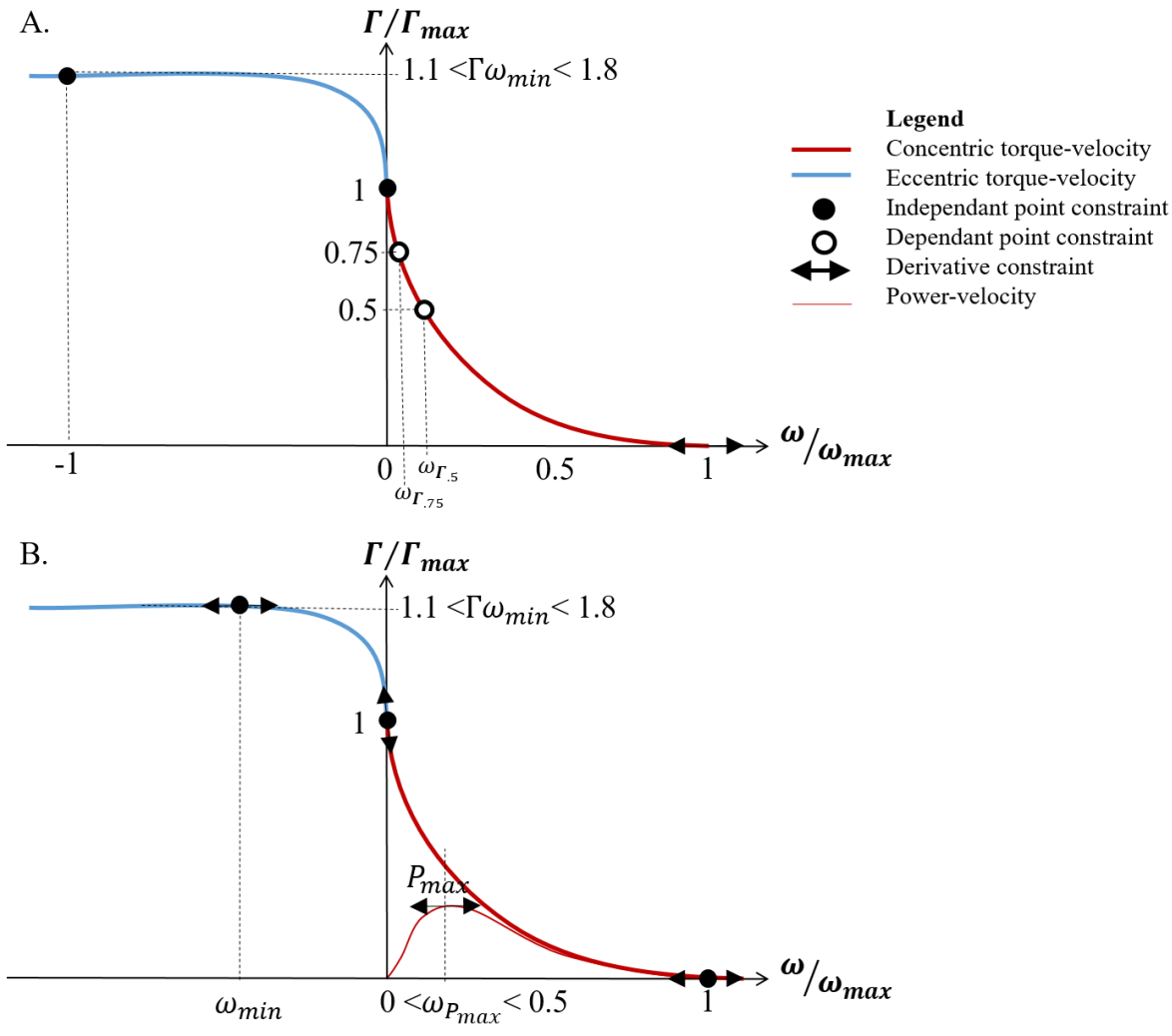

Figure 4 – Effects of torque-angle models (A) and interaction between the torque-angle and torque-velocity models (B) on mean errors computed as the average difference between maximal torque measured on the dynamometer and maximal torque predicted by the models. Colored stars represent individuals (one color = one subject). Black dots, blue dots and red diamonds represent the average of all individuals. Asterisks indicate significant difference between means.

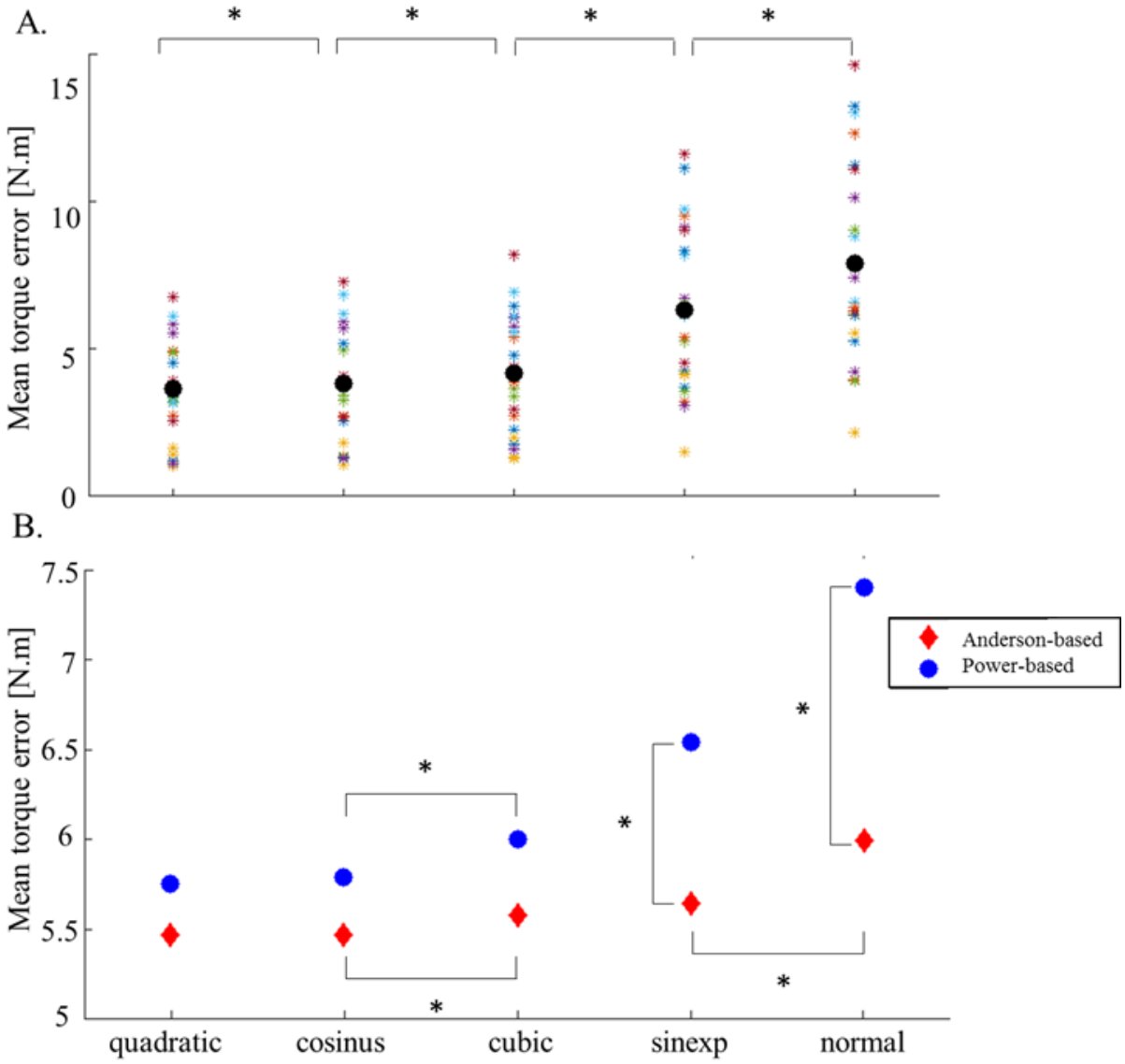

421 Table 1. Adjusted correlation coefficients between measured and predicted maximal
422 torque for all models in elbow flexion and extension for each type of data: isometric,
423 concentric and eccentric.

R^2			Normal	Cosinus	Quadratic	Cubic	Sinus-exponential
Anderson-based model	*flexion*	Isometric	.62	.86	.87	.84	.74
		Concentric	.58	.62	.62	.61	.61
		Eccentric	.75	.75	.75	.74	.77
	extension	Isometric	.66	.88	.89	.87	.75
		Concentric	.74	.75	.75	.76	.74
		Eccentric	.71	.77	.77	.76	.74
Power-based model	*flexion*	Isometric	.62	.86	.87	.84	.74
		Concentric	.64	.70	.70	.68	.68
		Eccentric	.60	.64	.64	.62	.64
	extension	Isometric	.66	.88	.89	.87	.75
		Concentric	.81	.85	.85	.85	.82
		Eccentric	.64	.70	.70	.70	.67

424

425 Table 2. Optimal elbow torque-angle parameters obtained with the five isometric models.

426 Values displayed in the table correspond to: means ± standard deviations.

		Normal	Cosinus	Quadratic	Cubic	Sinus-exp
FLEXION	$\boldsymbol{\Gamma_{max}}$ [N.m]	69 ± 13	63 ± 11	63 ± 11	64 ± 11	66 ± 12
	$\boldsymbol{RoM}$ [°]	175 ± 17	160 ± 33	155 ± 34	167 ± 28	173 ± 24
	$\boldsymbol{\alpha_0}$ [°]	79 ± 10	77 ± 13	77 ± 14	102 ± 12	59 ± 10
EXTENSION	$\boldsymbol{\Gamma_{max}}$ [N.m]	66 ± 18	60 ± 16	60 ± 16	61 ± 17	64 ± 18
	$\boldsymbol{RoM}$ [°]	179 ± 4	167 ± 27	164 ± 30	169 ± 23	173 ± 20
	$\boldsymbol{\alpha_0}$ [°]	76 ± 9	72 ± 11	72 ± 11	99 ± 10	56 ± 9

427
428

Table 3. Optimal elbow torque-velocity parameters of the new model obtained with the five isometric models. Values displayed in the table correspond to: means ± standard deviations.

Torque-angle model		Normal	Cosinus	Quadratic	Cubic	Sinus-exp
FLEXION	ω_{max} [°.s^{-1}]	1268 ± 514	1517 ± 544	1531 ± 548	1492 ± 567	1331 ± 507
	ω_{min} [°.s^{-1}]	-173 ± 87	-301 ± 276	-369 ± 500	-330 ± 477	-238 ± 241
	$\omega_{P_{max}}$ [°.s^{-1}]	404 ± 231	495 ± 242	502 ± 500	490 ± 255	426 ± 225
EXTENSION	ω_{max} [°.s^{-1}]	1368 ± 647	1636 ± 747	1667 ± 754	1605 ± 738	1458 ± 683
	ω_{min} [°.s^{-1}]	-297 ± 329	-509 ± 464	-531 ± 482	-536 ± 530	-391 ± 410
	$\omega_{P_{max}}$ [°.s^{-1}]	432 ± 291	551 ± 343	563 ± 347	537 ± 337	473 ± 305

Table 4. Optimal elbow eccentric to concentric ratios obtained with Anderson-based model and the new model combined with each of the five isometric models. Values displayed in the table correspond to: means ± standard deviations.

			Normal	Cosinus	Quadratic	Cubic	Sinus-exp
FLEXION	$\Gamma_{ECC}/\Gamma_{CON}$	Anderson-based	1.17 ±0.07	1.18 ±0.08	1.18 ±0.08	1.18 ±0.08	1.18 ±0.08
		ω_{max}-based	1.16 ±0.15	1.20 ±0.21	1.20 ±0.22	1.20 ±0.21	1.17 ±0.16
EXTENSION	$\Gamma_{ECC}/\Gamma_{CON}$	Anderson-based	1.21 ±0.10	1.22 ±0.10	1.22 ±0.10	1.22 ±0.10	1.21 ±0.10
		ω_{max}-based	1.17 ±0.15	1.34 ±0.30	1.32 ±0.30	1.31 ±0.29	1.21 ±0.20

SUPPLEMENTARY MATERIAL

USING TORQUE-ANGLE AND TORQUE-VELOCITY MODELS TO CHARACTERIZE ELBOW MECHANICAL FUNCTION: MODELING AND APPLIED ASPECTS

Diane Haering, Charles Pontonnier, Nicolas Bideau, Guillaume Nicolas, Georges Dumont

submitted to Journal of Biomechanical Engineering.

For the purpose of concision, the mathematical models used in the paper are extensively presented here.

1. Joint Torque Angle Relationships (JTAR)

Normal [8] $$\Gamma(\bar{\alpha}) = e^{-\frac{1}{2}(6\bar{\alpha})^2} \quad (1)$$

Cosinus [12] $$\Gamma(\bar{\alpha}) = cos(\pi\bar{\alpha}) \quad (2)$$

Quadratic [9,15] $$\Gamma(\bar{\alpha}) = -4\bar{\alpha}^2 + 1 \quad (3)$$

Cubic [11] $$\Gamma(\bar{\alpha}) = \frac{27}{4}\bar{\alpha}^3 - \frac{27}{8}\bar{\alpha}^2 - \frac{27}{16}\bar{\alpha} + \frac{27}{32} \quad (4)$$

Sinus-exponential [13] $$\Gamma(\bar{\alpha}) = \frac{1}{2}sin(1.919\pi\, e^{\bar{\alpha}}) + \frac{1}{2} \quad (5)$$

In all of these models, the normalized maximal torque ($\boldsymbol{\bar{\Gamma} = \frac{\Gamma}{\Gamma_{max}}}$) depended on the maximal isometric torque and on the joint angle to optimal joint angle distance normalized by the maximal range of isometric force production ($\boldsymbol{\bar{\alpha} = \frac{\alpha - \alpha_0}{RoM}}$) as presented in table 1. Those models are shown in figure 1. All coefficients used for the normal, quadratic, cubic and sinus-exponential models were obtained by solving the system of equations expressing the following constraints:

$\boldsymbol{\bar{\Gamma}}(\bar{\alpha}_{\mathbf{0}}) = 1$,

$\boldsymbol{\bar{\Gamma}}(\bar{\alpha}_{\boldsymbol{min}}) = 0$,

$\boldsymbol{\bar{\Gamma}}(\bar{\alpha}_{\boldsymbol{max}}) = 0$, and

$\bar{\alpha}_{\boldsymbol{max}} - \bar{\alpha}_{\boldsymbol{min}} = \mathbf{1}$; $\bar{\alpha}_{max}$ and $\bar{\alpha}_{min}$.being normalized values of maximal and minimal angles.

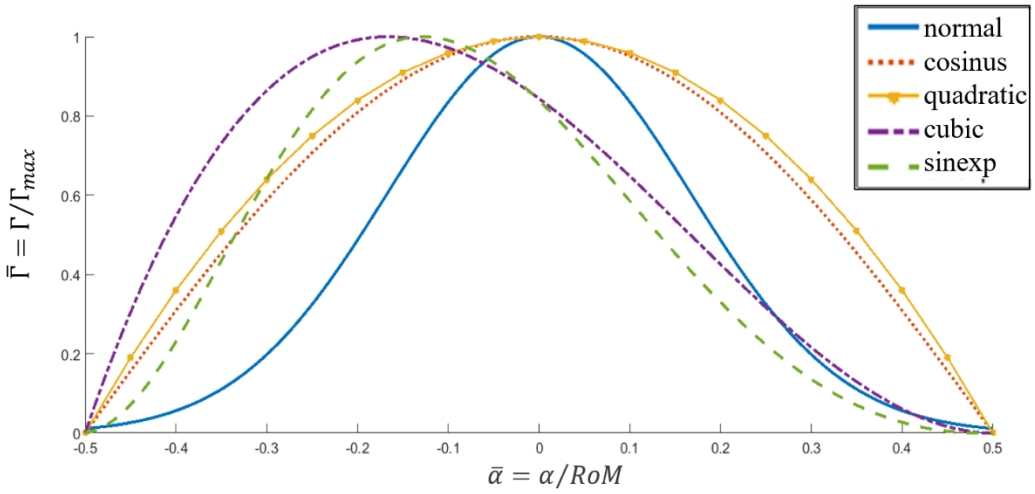

Figure 1 – Normalized torque-angle relationship as defined by the five mathematical models: normal, cosinus, and quadratic models are symmetrical; cubic and sinus-exponential are asymmetrical.

Table 1: JTAR parameters

Parameters		**Limits**	
Γ_{max}	Max. isometric torque	0.75 Γ_{meas}	1.25 Γ_{meas}
RoM	Max. isometric range of motion	0	π
α_0	Isometric optimal angle	$\pi/6$	$5\pi/6$

2. Joint Torque Velocity Relationships (JTVR)

2.1.JTVR parameters

This section presents the parameters exploited in the models presented below.

Table 2. JTVR parameters

Model	**Parameters**			**Limits**	
Anderson-based torque-velocity model	P_1	$\omega_{\Gamma_{.75}}$	Velocity at 75% of maximal isometric torque	0	π
	P_2	$\omega_{\Gamma_{.5}}/\omega_{\Gamma_{.75}}$	Ratio between velocities at 50% and 75% of maximal isometric torque	1.9	2.1
	P_3	E	Eccentric to concentric torque index	.1	.8
Power-based torque-velocity model	P_1	ω_{max}	Max. concentric velocity	$\pi/3$	5π
	P_2	$\omega_{P_{max}}$	Velocity at maximal power	0.25	0.4
	P_3	$\omega_{min}/\omega_{max}$	Max. eccentric to concentric velocity ratio	-1	-0.1
	P_4	$\Gamma_{ECC}/\Gamma_{CON}$	Max. eccentric to concentric torque ratio	1.1	1.8

2.2. Anderson-based model

$$\begin{cases} \Gamma(\omega) = \frac{2P_1P_2+\omega(P_2-3P_1)}{2P_1P_2+\omega(2P_2-4P_1)}, & \boldsymbol{\omega \geq 0} \\ \Gamma(\omega) = \left(\frac{2P_1P_2+\omega(P_2-3P_1)}{2P_1P_2+\omega(2P_2-4P_1)}\right)(1-P_3\omega), & \boldsymbol{\omega < 0} \end{cases} \quad (1)$$

where P_1 is the velocity at 75% of maximal isometric torque, P_2 is the ratio between velocities at 50% and 75% of maximal isometric torque, and P_3 is a maximal eccentric to maximal concentric torque index.

2.3.Power-based torque-velocity model

$$\begin{cases} \Gamma(\bar{\omega}) = 0, & \mathbf{1} \le \bar{\boldsymbol{\omega}} \\ \Gamma(\bar{\omega}) = a_1\bar{\omega}^3 + b_1\bar{\omega}^2 + c_1\bar{\omega} + d_1, & \mathbf{0} \le \bar{\boldsymbol{\omega}} < \mathbf{1} \\ \Gamma(\bar{\omega}) = a_2\bar{\omega}^3 + b_2\bar{\omega}^2 + c_2\bar{\omega} + d_2, & \boldsymbol{P_3} \le \bar{\boldsymbol{\omega}} < \mathbf{0} \\ \Gamma(\bar{\omega}) = P_4, & \bar{\boldsymbol{\omega}} < \boldsymbol{P_3} \end{cases} \quad (2)$$

with:

$$\bar{\omega} = \frac{\omega}{P_1},$$

$$a_1 = -\frac{3{P_2}^2 - 4P_2 + 1}{4{P_2}^3 - 6{P_2}^2 + 2P_2},$$

$$b_1 = \frac{2{P_2}^3 - 3P_2 + 1}{2{P_2}^3 - 3{P_2}^2 + P_2},$$

$$c_1 = \frac{8{P_2}^3 - 9{P_2}^2 + 1}{4{P_2}^3 - 6{P_2}^2 + 2P_2},$$

$$d_1 = 1,$$

and

$$a_2 = -\frac{P_3 - 4P_2 - 9{P_2}^2P_3 - 12{P_2}^2P_4 + 8{P_2}^3P_3 + 8{P_2}^3P_4 + 12{P_2}^2 - 8{P_2}^3 + 4P_2P_4}{2{P_3}^3\left(2{P_2}^3 - 3{P_2}^2 + P_2\right)},$$

$$b_2 = \frac{2{P_2}^3 - 3P_2 + 1}{2{P_2}^3 - 3{P_2}^2 + P_2},$$

$$c_2 = \frac{8{P_2}^3 - 9{P_2}^2 + 1}{4{P_2}^3 - 6{P_2}^2 + 2P_2},$$

$$d_2 = 1,$$

where P_1 is the maximal concentric velocity, P_2 is the velocity at maximal power, P_3 is maximal eccentric velocity to maximal concentric velocity ratio, and P_4 is the maximal eccentric to maximal concentric torque ratio.

2.4. Model representations

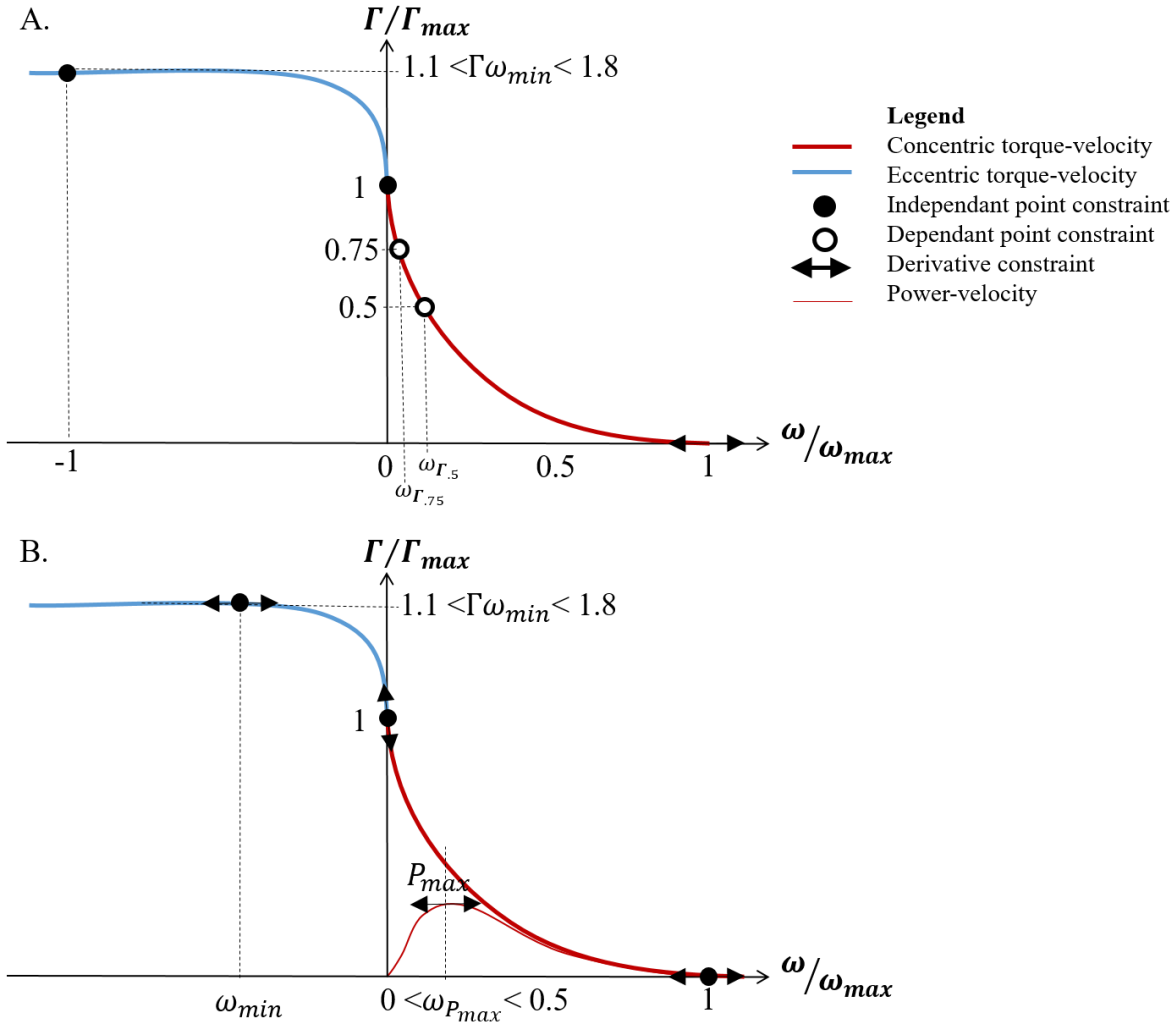

Figure 2 – Normalized torque-velocity models and constraint parameters: in the Anderson-based model (A), we find one derivative constraint at ω_{max}, two independent constraints at $-\omega_{max}$ and ω_0, and two dependant constraints at $\omega_{\Gamma.5}$ and $\omega_{\Gamma.75}$; in the power-based model (B), we defined three derivative constraints and three independent constraints at ω_{max}, ω_{max}, and ω_0, and an additional derivative constraints at $\omega_{P_{max}}$ on the power-velocity relationship.

3. Visualization of model to measurement fitting

3.1. Joint Torque Angle Relationships

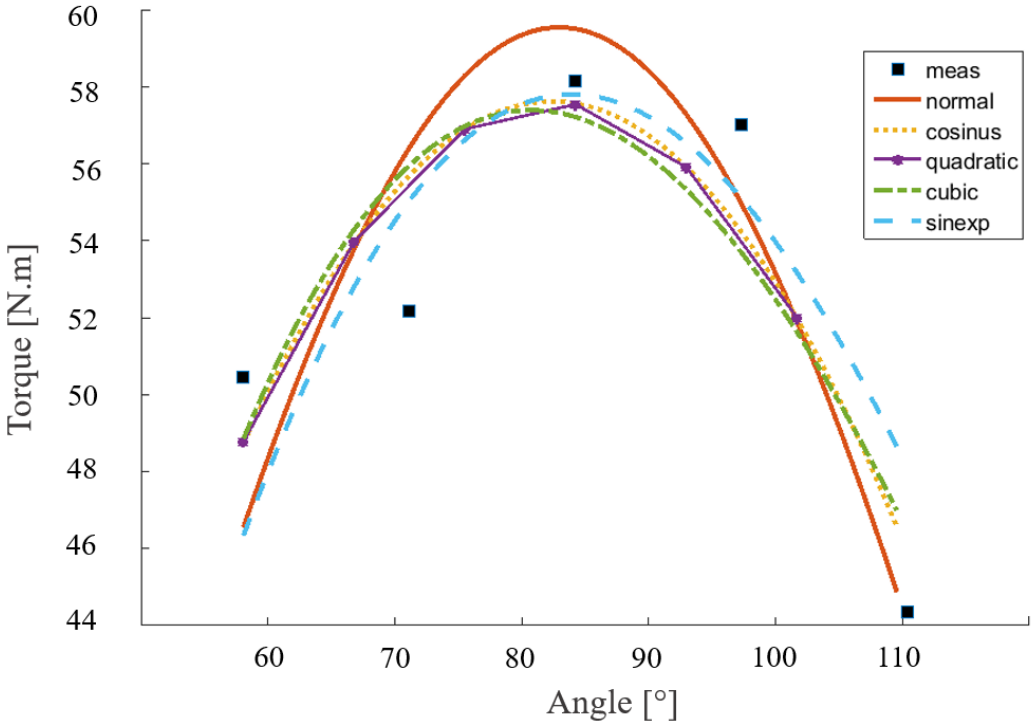

Figure 3 – Example of comparison between normal, cosines, quadratic, cubic and sinus exponential JTAR models fitting on isometric maximum torque measurements (black squares).

3.2. Joint Torque Angle & Joint Torque Velocity Relationships

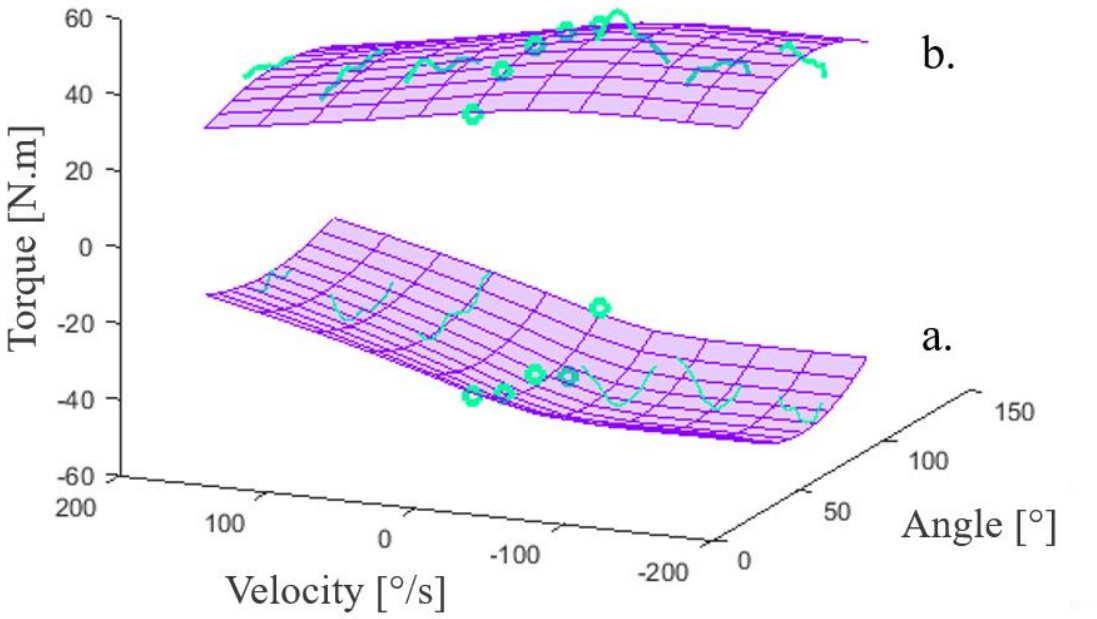

Figure 4 – Example of a combined JTAR and JTVR model mesh fitting on isometric maximum (dots) and isokinetic (lines) torque measurements for a. elbow flexion, and b. elbow extension.